

Structure of Polymer Brushes in Cylindrical Tubes: A Molecular Dynamics Simulation

Dimitar I. Dimitrov¹, Andrey Milchev^{2,3}, Kurt Binder³, and Dieter W. Heermann⁴

¹ Inorganic Chemistry and Physical Chemistry Department, University of Food Technology, 26 Maritza Blvd., 4002 Plovdiv, Bulgaria

² Institute of Physical Chemistry, Bulgarian Academy of Sciences, 1113 Sofia, Bulgaria

³ Institut für Physik, Johannes Gutenberg Universität Mainz, Staudinger Weg 7, 55099 Mainz, Germany

⁴ Institut für Theoretische Physik, Universität Heidelberg, Philosophenweg 19, 69120 Heidelberg, Germany

February 7, 2022

Abstract

Molecular Dynamics simulations of a coarse-grained bead-spring model of flexible macromolecules tethered with one end to the surface of a cylindrical pore are presented. Chain length N and grafting density σ are varied over a wide range and the crossover from “mushroom” to “brush” behavior is studied for three pore diameters. The monomer density profile and the distribution of the free chain ends are computed and compared to the corresponding model of polymer brushes at flat substrates. It is found that there exists a regime of N and σ for large enough pore diameter where the brush height in the pore exceeds the brush height on the flat substrate, while for large enough N and σ (and small enough pore diameters) the opposite behavior occurs, i.e. the brush is compressed by confinement. These findings are used to discuss the corresponding theories on polymer brushes at concave substrates.

1 Introduction

By special endgroups flexible macromolecules can be tethered to a substrate via its chain end. In a dilute solution under good solvent conditions using a non-adsorbing substrate surface that repels the monomers one thus obtains a “mushroom” configuration of the polymer [1, 2]. If one grafts many such polymer chains on the substrate, such that the polymer coils in their mushroom configuration would strongly overlap each other, excluded volume interactions reduce this overlap by leading to strongly stretched configurations of the coils, the so-called “polymer brushes” [2, 3]. In this way, the substrate is coated with a polymeric layer of height h proportional to the chain length N of these endgrafted polymers [2, 3, 4, 5]. Of course, the distinction between “mushrooms” and “brushes” is not a completely sharp one, but rather these states of a surface coated by endgrafted polymers are separated by broad crossover regime where the coils overlap weakly and get more and more stretched as with increasing grafting density the overlap increases.

Since such polymer brushes find important applications such as colloid stabiliza-

there has been an enormous interest in these systems, ranging from various methods of their synthesis [6] to their theoretical understanding by analytic theory [2] - [4], [7] - [25] and computer simulation [26] - [39]. Most of this work concerns polymers tethered to flat planar substrates, however, and brushes on curved substrates were considered only occasionally [10, 17, 21, 22, 23, 24, 25, 30, 35, 36, 39] although this case clearly is relevant in practice, too. Since it was stated that brushes adsorbed on the outside of spherical or cylindrical surfaces differ in many interesting aspects from flat brushes [17], while brushes at the inside of spheres or cylinders were claimed to differ relatively little from the planar substrate case [17], not much attention was paid to brushes grafted to the surface of spherical [22, 25, 35] or cylindrical [10, 22, 25, 39] pores. While it is clear that such a brush gets compressed when the pore diameter D becomes comparable to the height h , the brush would adopt under otherwise identical conditions, conflicting predictions appear in the literature concerning the behavior for large D : while the Sevick theory [22] suggests that the brush height is maximal for $D \rightarrow \infty$ and decreases monotonously with $1/D$, self-consistent field arguments [10, 25] imply that for small $1/D$ the brush expands slightly. No simulations have so far been carried out for brushes in cylindrical pores yet at all, apart from a study of electroosmotic flow in capillaries and its control by endgrafted chains [39] (this work was restricted to a single chain length $N = 10$ and the mushroom regime, however).

In the present paper, we wish to fill this gap by presenting Molecular Dynamics simulations of polymer brushes in cylindrical pores, and hence present numerical evidence to settle this issue whether brushes on weakly concave substrates shrink or expand, in comparison with the flat case.

2 Model and Simulation Method

The present study does not concern a chemically realistic description of a specific polymer, but rather we are interested in the generic features of polymer brushes grafted inside of cylindrical tubes only. Therefore we disregard any details of chemical structure, and work with a coarse-grained bead-spring model only. The beads hence represent effective monomeric units, as usual, like Kuhn segments, so the nearest-neighbor distance along a bead-spring chain does not correspond to a chemical bond between carbon atoms ($\approx 0.15nm$) but rather is of the order of $1nm$. On this scale, the effects of the torsional and bond-angle potentials can be considered to be averaged out, and all what is left is an effective interaction between monomeric units and an effective spring potential between neighboring monomeric units (beads) along the chain [40, 41, 42, 43, 44]. There is ample evidence that such models are useful to describe many properties of macromolecular systems [40, 41, 42, 43, 44], and in fact previous work on simulation of polymer brushes on flat substrates [26, 27, 31, 34, 36, 38, 45] and on the outside of nanocylinders [30] have used such models successfully.

The interactions between the beads are then modeled by a Lennard-Jones (LJ) potential $U_{LJ}(r)$ that is truncated at r_c and shifted to zero there to avoid a singularity in the force,

$$U(\vec{r}_i - \vec{r}_j) = U_{LJ}(r) - U_{LJ}(r_c), \quad r = |\vec{r}_i - \vec{r}_j|, \quad (1)$$

$$U_{LJ}(r) = 4\epsilon[(\sigma_{mm}/r)^{12} - (\sigma_{mm}/r)^6], \quad (2)$$

where \vec{r}_i is the position of the i 'th bead, the parameters ϵ and σ_{mm} set the scales for the strength and range of the LJ potential, and the cutoff distance r_c is chosen as

Note that most previous work on polymer brushes (apart from [31, 38, 45]) have truncated and shifted the potential right in its minimum, i.e. choosing $r_c = 2^{1/6}\sigma_{mm}$ rather than Eq. (3), and then the potential is purely repulsive. Such an almost athermal model can describe a polymer brush under conditions of a very good solvent only, but it would not be possible to consider brushes under conditions of a bad solvent or under Theta-conditions [46]. For the model defined in Eqs. (1), (2), (3) the Theta temperature Θ has been estimated as [47] $k_B\Theta/\epsilon \approx 3.3$. In the present work, we study polymer brushes under conditions of a (moderately) good solvent only, choosing the temperature of the simulation throughout as $k_B T/\epsilon = 4.0$, following [38]. The spring potential is created by adding a finitely extensible nonlinear elastic (FENE) potential [48]

$$U_{FENE}(r) = -15\epsilon(R_0/\sigma_{mm})^2 \ln(1 - r^2/R_0^2), \quad R_0 = 1.5\sigma_{mm}, \quad (4)$$

to Eq. (1) if monomers i, j are nearest neighbors along a chain. The choice of the additional parameters that appear in Eq. (4) ensure that there is no tendency for the beads to form a simple crystal structure (face-centered cubic or body-centered cubic, for instance) at high density, because the minimum of the potential for two bonded monomers (neighbors along a chain) occurs at $r_{min} \approx 0.96\sigma_{mm}$, rather different from (and incommensurate with) the minimum distance of $U_{LJ}(r)$, $r_{min} \approx 1.12\sigma_{mm}$. Therefore the present model at low temperatures, T far below Θ , freezes into a glass-like structure, both for ordinary melts [49] (i.e., chains that are not grafted to a substrate) and for polymer brushes [50]. However, studies of the present model of a polymer brush in a cylinder at and below the Theta temperature will be left to future work.

The grafting wall is represented by particles forming a triangular lattice, wrapped on a torus by a periodic boundary condition, and choosing the triangular lattice spacing and the number of wall particles such that a cylinder of diameter D results. The particles forming this cylindrical wall are bound together by the same potential as the spring potential between the beads of the chain, defined by Eqs. (1)-(4). Thus it is ensured (through the repulsive part of the potential, Eq. (2)) that no bead can cross the cylinder surface, at the temperatures of interest, to get out of the cylinder. In the direction along the straight cylinder axis, the standard periodic boundary condition is taken, as usual. The grafted chain ends of the polymers are put on regular positions of a lattice on the surface of a cylinder whose radius is one length unit smaller than the cylinder forming the confining tube.

This choice of cylindrical confinement is computationally convenient and in fact was motivated by the research on carbon nanotubes [51]. However, it should be noted that by techniques such as combinations of electron beam lithography and nanoimprint lithography artificial nanochannels can be fabricated with a width between $35nm$ and $150nm$ [52], and such nanochannels were recently used to study statics and dynamics of confined DNA macromolecules [53]. Thus a different modeling of the walls of the confining tube may be appropriate for such artificial nanochannels, but this is left to later work. Still a different modeling may be required to describe confinement of grafted biopolymers in cylindrical pores in biological membranes, however.

Particular care is needed to create an initial configuration of the grafted polymers and equilibrate it. Periodically arranged grafting sites are chosen simply to be the wall particles, according to a chosen grafting density σ . Choosing our units of length and temperature such that $\sigma_{mm} = 1, \epsilon = 1, k_B \equiv 1$, we work with cylindrical diameters $D = 30, 42$, and 62 , the corresponding lengths of the cylinders in the direction of the cylinder axis being $L = 81.61, 76.18$, and 67.47 , respectively. For comparison, also brushes on flat substrates were studied (formally this corresponds

of equilibration, for $D = 30$ the maximum chain length that could be studied was $N = 64$, for $D = 42$ we could go up to $N = 80$, and for $D = 60$ up to $N = 112$, at the smallest grafting density studied, and $N = 24, 32$ and 64 , at the largest grafting densities used for $D = 30, 42$ and 62 , respectively. At the highest grafting densities studied, the cylindrical tubes were already filled uniformly with monomeric units at melt density. If the grafting density is lower than its maximal value, or the chain length shorter, an empty region free of monomeric units remains present near the axis of the cylindrical channel (Fig. 1), and this free volume facilitates equilibration.

Next we describe the construction of the initial configuration of the grafted polymers. This construction begins for a given (N, σ, R) with the growth of chains in a tube with radius $R_{init} = 2R$ and $N = N_{max}$, where N_{max} is the number of monomers in the longest chain investigated for this choice of σ and R . After the first monomer has been placed at the grafting site, each subsequent monomer is put at a point at distance $0.075R_0$ from the previous one, along a direction $\vec{r} = 2.0 * \vec{e}_{0z} + \vec{e}_{rand}$, \vec{e}_{0z} being a unit vector pointing radially from the grafting site to the tube axis (i.e., along the z -axis), while \vec{e}_{rand} is another unit vector oriented at random. After an initial equilibration of this system for about 10^5 MD steps, the tube radius is rescaled to the desired final value R , and again the system is equilibrated for 10^5 MD steps. From the final configuration of this system, several systems with different values of N are created, by cutting of the monomers near the free chain end consecutively and eliminating them. These systems then are further equilibrated for about $3 \cdot 10^5$ MD steps. These then are the starting configurations for the averaging process (typically statistics is collected during runs lasting from $2 \cdot 10^5$ to $4 \cdot 10^5$ MD steps). Equilibration was done by Molecular Dynamics (MD), applying the standard leapfrog algorithm [42], keeping the temperature constant via the Nose-Hoover thermostat [42]. Choosing the mass of an effective monomer as $m = 1$, the MD time unit is $t_0 = (\sigma_{mm}^2 m / 48\epsilon)^{1/2} = 1/\sqrt{48}$, and the integration time step then is chosen as $\delta t = 0.0005 t_0$. Always 10^6 MD steps were discarded for equilibration before averages were taken. In this paper, we focus on our results on the density profiles of the effective monomers and of the free chain ends, while corresponding data on the chain extensions parallel and perpendicular to the tube axis will be analyzed elsewhere [54].

3 Density Profiles and Chain End Distributions in Confined Cylindrical Brushes

Figs. 2 - 5 show a representative selection of our simulation results, displaying in the upper part the brush density profile and in the lower part the corresponding radial distribution of free chain ends, both for a number of chain lengths N for the chosen combination of parameters D and σ , respectively. This is only a small subset of all the data that have been generated. Here $\phi(r)$ is the number density of monomers in a radial shell between r and $r + dr$, normalized such that $2\pi L \int_0^{\frac{D}{2}} r dr \phi(r)$ yields the total number of monomers in the system, and the end monomer distribution $\rho(r)$ is defined accordingly.

It is seen that for small N , ($N \leq 16$), in all cases the behavior of these distribution functions is typical of polymer mushroom behavior, as it is recalled in part (a) of Fig.5 for a polymer brush at a planar grafting surface, but choosing σ so small that the chains are essentially noninteracting. Then one still finds a small-scale structure in $\phi(r)$, due to the nearest and next nearest neighbors of the grafting site (counted along the chain) which is absent in the end monomer distribution of course. But

both $\phi(r)$ and $\rho(r)$ have a broad peak of comparable width and a similar decay to zero at large distances from the grafting site.

When the chain length N (and — or the grafting density σ) gradually increases one observes a smooth crossover of the distributions $\phi(r)$ and $\rho(r)$ to a behavior that is typical for polymer brushes on flat substrates. The behavior is completely different for large chains and/or high grafting densities: then the monomer density becomes uniform throughout the cylinder, apart from the immediate neighborhood of the grafting surface, and the end monomer distribution gets peaked in the cylinder axis region. There is, however, a smooth - almost linear - decay of this end monomer distribution towards the grafting surface: thus the approximation of this distribution by a delta function obviously is very inaccurate. When one compares these density profiles in cylindrical tubes (Figs. 2 - 4) to the corresponding density profiles of brushes at flat substrates, one notes great similarity between both cases near the grafting surfaces. In the outer region of the brushes, however, the behavior is markedly different: for a brush on a flat surface extending into the half space, near the outer boundary of the brush (i.e., near $z = h$ where h is the “brush height” [3, 4]) there is a slow and gradual decay of all profiles towards zero. For the brush in the cylinder, however, this is not the case: at $r = 0$ both $\phi(r)$ and $\rho(r)$ reach nonzero limits, for long enough chains and/or high enough grafting densities. When we continue to call such a state of endgrafted polymers in a cylindrical tube a ”brush” we do not imply anything about the stretching of the chains, of course. In addition one must consider the possibility that monomers of a chain are anywhere inside of the cylinder, and hence they are not confined to the semi-cylinder where the grafting point is located, but also in the opposite semi-cylinder. Thus when we introduce an orthogonal coordinate system such that the origin coincides with the grafting site of a chain, the y -axis running within the cylinder surface parallel to the cylinder axis, and the z -axis runs perpendicular towards the cylinder axis, monomers of long enough chains (in particular the chain ends), may have z -coordinates in the full range $0 < z < D$ and not only in the range corresponding to the hemicylinder containing the grafting point at its bottom, $0 < z < D/2$. In the cylindrical coordinate system one chooses the center of the coordinate system in the cylinder axis, however, and r is the radial distance from the cylinder axis. We have two inequivalent entries for the same r , namely

$$r' = D/2 - r, \text{ for } z < D/2, \text{ and } r' = r + D/2, \text{ for } z > D/2 \quad (5)$$

The information which monomers are in the upper semicylinder and which are in the lower semicylinder is lost when one uses the simple cylindrical coordinates, as done in Figs. 2 - 4. However, we have nevertheless given this information, since it is a standard assumption of the theoretical treatments that chains are confined to the semicylinder $z < D/2$, or even the stronger assumption is made that chains are confined to a cone, the cone axes running from the grafting site along the z -axis with the cone top being in the cylinder axis [22, 25], the opening angle of the cone being controlled by the grafting density via an adaptation of the Alexander - de Gennes blob picture [1, 2, 3] to the cylindrical geometry. Our results imply that such a picture is by far too restrictive, however.

Figs. 6 - 9 now give the corresponding distributions of the monomer density $\phi(r')$ and the chain ends $\rho(r')$ for a number of typical cases. It is clearly recognized that the monomers are not restricted to the region $r' < D/2$, and actually the distributions at the distance $r' = D/2$ corresponding to the cylinder axis are perfectly smooth. In this coordinate system where the full range $0 < r' < D$ is considered, the distributions are again rather similar to the corresponding profiles of brushes grafted to flat substrates ($D \rightarrow \infty$).

The profiles $\phi(r')$ have now been used to compute the first moment $\langle r' \rangle$ and from $\langle r' \rangle$ one can estimate the brush height h as $h = 8\langle r' \rangle/3$ (Note that the (somewhat arbitrary) factor $8/3$ is motivated by using the parabolic density profile predicted by the strong stretching limit of the self-consistent field theory for brushes at flat substrates, although the actual profiles are rather different, as Figs. 6 - 9 show. But we use this factor $8/3$ so that our results for h in the case of flat brushes conform to the results that one can find in the literature.):

$$h = \frac{8}{3}\langle r' \rangle, \quad \langle r' \rangle = \frac{\int_0^D r' \phi(r') dr'}{\int_0^D \phi(r') dr'} \quad (6)$$

For brushes on flat substrates one has the well known property $h \propto N$ for large enough N . For brushes on cylindrical substrates with small enough D the brushes are compressed and hence a weaker increase is expected. However, one expects from the self-consistent field theory that for not too large N (or large enough D , respectively, such that the center of the cylinder is still more or less free of monomers, cf. Fig 1) that the density profile of a brush decreases somewhat slower in a cylindrical brush than for the corresponding blobs in a brush on the flat substrate, under identical conditions. For the "blobs" close to the cylinder axis, less volume is available than for corresponding blobs in a brush on a flat substrate. As a consequence, a correspondingly stronger stretching tendency for chains in a blob grafted to the inner surface of the cylinder would be predicted. Our numerical results for brushes in cylinders with large enough D (Fig. 10) are comparable with this prediction and with numerical results obtained by the SCMF (self consistent mean field) theory of Szleifer and Carignano [35]. Hence, the theoretical result of Sevick [22] that the brush height is longest for $D \rightarrow \infty$ and decreases monotonously while decreasing D is not confirmed by our simulations. Of course, this trend seen on Fig. 10 cannot hold indefinitely with increasing N . Of course, Sevick theory [22] is based on the Alexander-de Gennes ansatz that the end monomers are localized at $r = h$ (for a flat brush this implies a delta function density profile $\phi(r)$), and thus it is not surprising that this theory is inaccurate.

When all the free volume in the center of the brush (Fig. 1) is filled up with monomers, compression of the brush sets in, and consequently the monomer density gets enhanced also in the region of the brush close to the cylinder walls. In this regime, we expect that the height of a brush on a flat substrate would be larger than the height of the brush, confined into the cylinder, and this is nicely demonstrated for a narrow enough tube in Fig. 10 too. Of course, when there is no longer any region free of monomers left near the center of the tube, the notions of "polymer brush" and "brush height" lose their meaning. In fact, rather than comparing polymer brushes one may encounter states where the chain conformations rather resemble "cigars", i.e. they are elongated along the axis of the pore.

4 Conclusions

In this paper, a first exploratory investigation of the structure of a brush confined in cylinders of various diameters by means of Molecular Dynamics computer simulations has been presented, using a (coarse-grained) bead-spring model under conditions of moderately good solvent (but without taking the solvent particles into account explicitly - the effect of the solvent thus is described only with respect to static thermodynamic and structural properties, while the effect on dynamic properties, e.g. via mediating the hydrodynamic interactions, is missing). The walls

prevent the escape of any monomer towards the outside. The parameters of the problem (chain length N , grafting density σ , cylinder diameter D) are varied and a comparison with the properties of the corresponding brush model on a flat substrate is also made.

In analysing the monomer and chain end density, it is suggested that one needs to consider normally the standard radial density profiles $\phi(r), \rho(r)$, but one may consider a complementary coordinate r' , which uses the information where the anchor point of the chain is: We define $r' = D/2 - r$ when the considered monomer is in the same "hemicylinder" as the anchor point, while $r' = D/2 + r$ when the monomer is in the other "hemicylinder" (cf. the analogous profile of chains grafted inside a sphere: taking the grafting site of a chain as the south pole, it makes a difference whether the monomer is in the southern or northern hemisphere). Then the profiles are smooth also at $r' = D/2$, corresponding to $r = 0$, see Figs. 6 - 8, and resemble that of a brush on a flat substrate (Fig. 5).

On the other hand, the standard radial density profile (Figs. 2 - 4) is rather different as soon as the central part of the cylinder is no longer empty (Fig. 1), since then at $r = 0$ the densities happen to be nonzero and the similarity with the case of brushes on flat surfaces is lost. That difference is reminiscent to the case of density profiles when two brushes on planar surfaces are brought together to such a small distance D that they start to interpenetrate. One still can ask a question what is the density profile of the monomers (or chain ends) of the left brush also at distance $z > D/2$ and likewise for the monomers (or chain ends) of the right brush (grafting sites near $z = D$ at distances $z < D/2$). This information on the interdigitation of the chains from the two brushes is of critical importance when one considers dynamical behavior (e.g. when shear is applied). Likewise, we feel that Figs. 6 - 8 contain an important structural information that will play a role when one discusses the flow of particles through the cylinder along its axis (we shall investigate this problem in future work).

One aspect that has been discussed contradictorily in the literature is the effect of cylindrical confinement on the height of the brush - while the theory of Sevick predicted that the maximal brush height occurs for the flat substrate, and with increasing inverse radius of cylinder $1/R$ the height of the brush decreases monotonously other arguments suggest that for small $1/R$ the brush height increases first and decreases later, when a regime of compressed brush is reached, where no longer any free volume near the center of the cylinder is left. Our results are comparable with the latter picture, although the change of the brush profile (and the brush height) is rather small for small $1/R$.

Our results for the profiles of the monomer density and the chain ends (Figs. 6 - 8) also imply that the monomers of a chain are *not* confined to a conical sector of the cylinder with the cone top in the cylinder axis, as suggested by simple generalizations of the Alexander-De Gennes blob picture [2, 3] for flat brushes to the cylindrical geometry [16, 25] (Fig. 11). Presumably for entropic reasons, it is much more favorable if a much larger part of the cylinder volume is shared by many grafted chains, rather than dividing up the cylinder into separate conical "compartments" each containing a single chain. This finding is not really a surprize since the Alexander-De Gennes blob picture is known to be rather unreliable also for brushes on flat substrates, see e.g. [32, 33].

There are many directions into which our study could be generalized: Obvious generalizations include the study of dynamic correlations and response to external perturbations. Of particular interest, both in nanotechnology and for biological application would be to consider the transport of various molecules or nanoparticles. It is conceivable that such a transport is either easily possible or very difficult or even

the fact that arrays of cylindrical nanotubes with various diameters can be fabricated and used for various experiments, it is also hoped that the present study will stimulate continuing experimental work on brushes in such cylindrical geometries.

5 Acknowledgments

Support from the Deutsche Forschungsgemeinschaft (DFG) under project No 436 BUL 113/130 is gratefully acknowledged. One of us (D.I.D.) thanks the Max-Planck society for support via a Max-Planck Fellowship during the time this paper was completed.

Figure 1: Snapshot picture of a brush grafted inside of a cylinder, for $N = 16$, $D = 30$, $\sigma = 0.08$, displaying different chains in distinct colors in order to be able to distinguish them. Top shows a side view of the cylinder, lower part a view of the cross section. Note that the particles forming the cylindrical wall are not displayed.

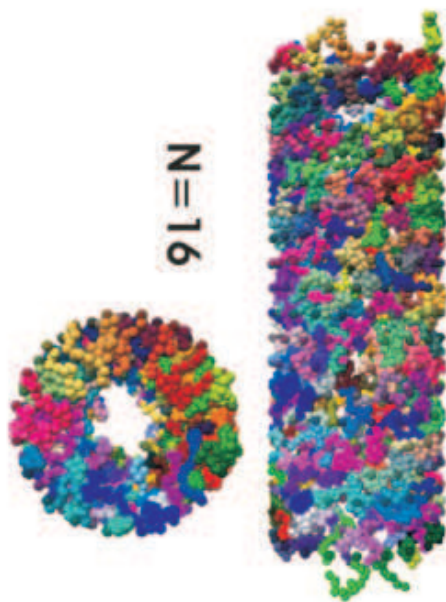
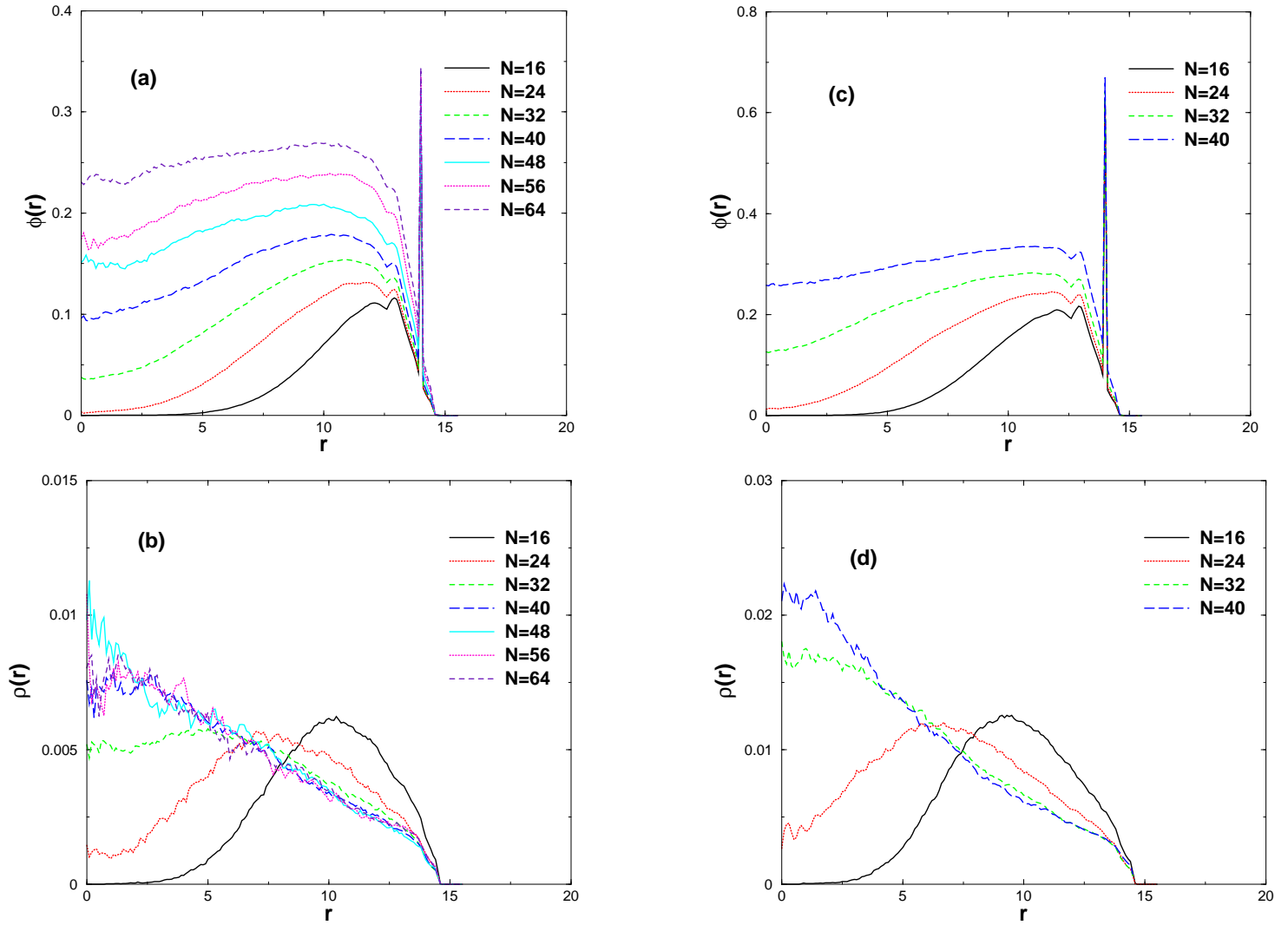


Figure 2: Radial distribution of the density $\phi(r)$ of monomeric units (upper part) and of the free chain ends $\rho(r)$ (lower part) plotted vs the radial distance r from the cylinder axis, for a cylindrical tube of diameter $D = 30$. Note that the sharp peak in $\phi(r)$ represents the first monomer of the grafted chains at the fixed distance $\Delta r = 1$ from the atoms forming the cylindrical wall. Part (a,b) refers to $N_{ch} = 196$ ($\sigma = 0.02730$) and part (c,d) refers to $N_{ch} = 400$ ($\sigma = 0.05572$).



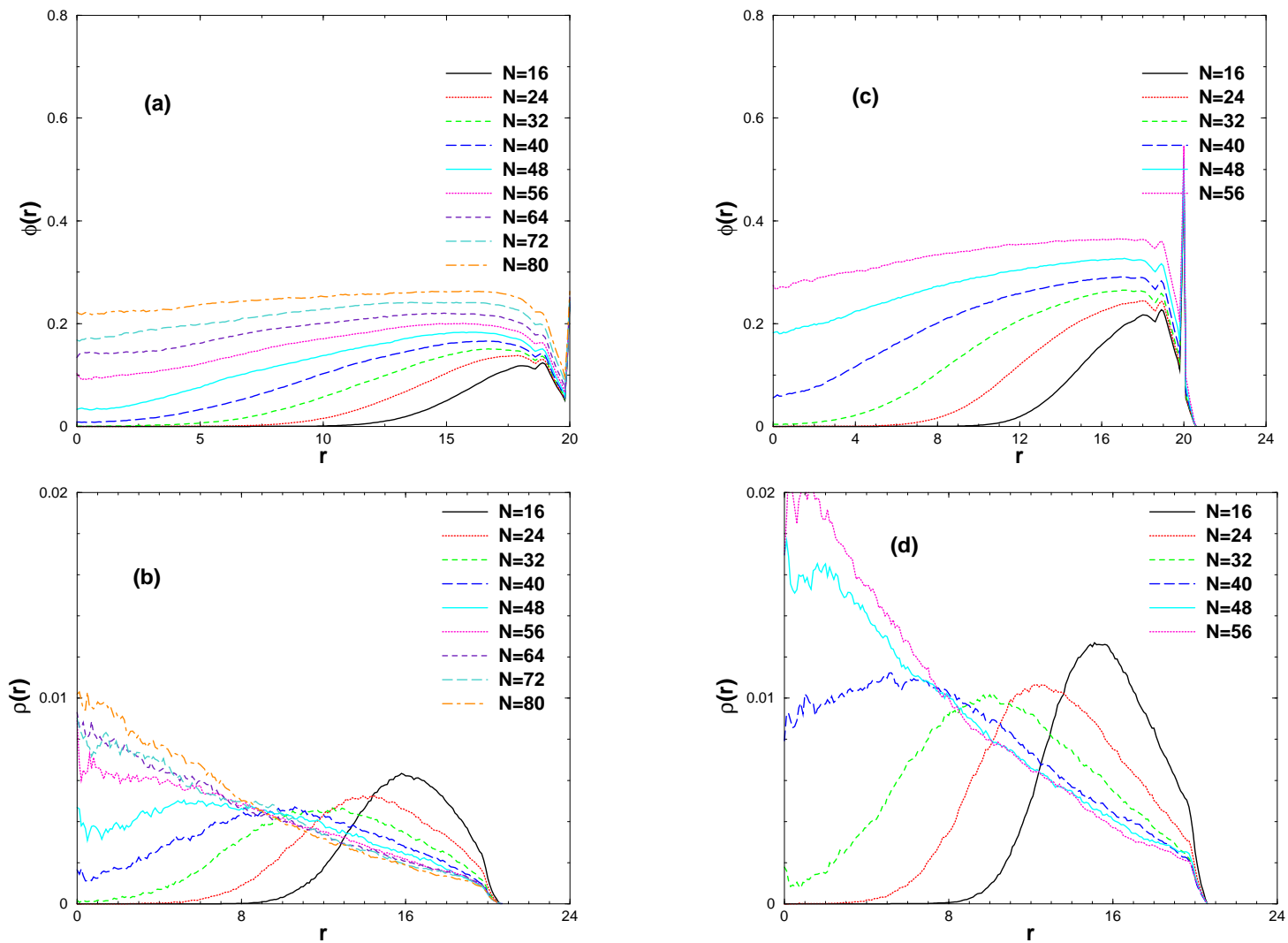
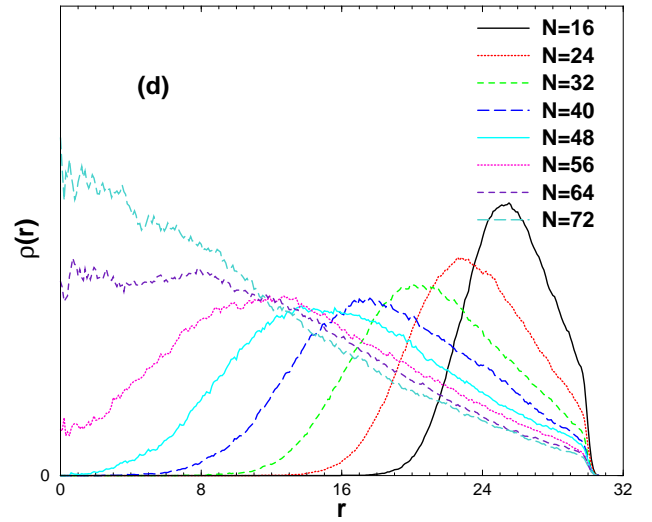
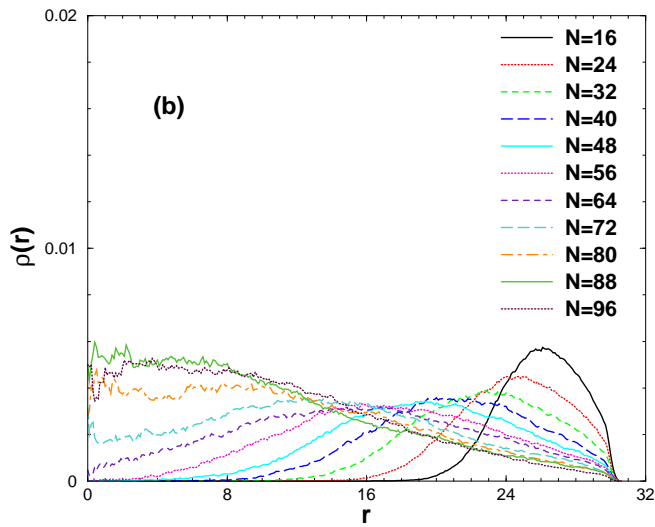
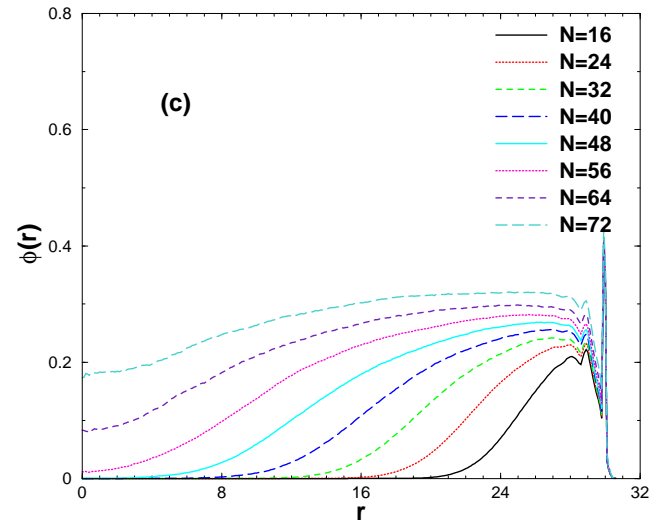
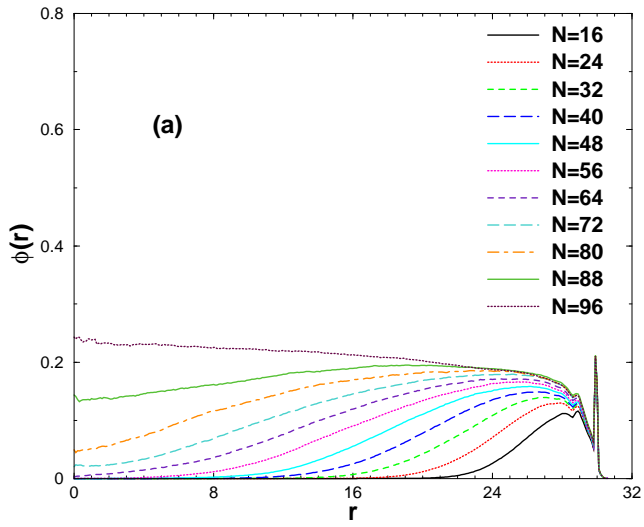


Figure 3: Same as Fig. 2, but for $D=42$. Part (a,b) refers to $N_{ch} = 294$ ($\sigma = 0.03071$) and part (c,d) refers to $N_{ch} = 600$ ($\sigma = 0.06268$)

Figure 4: Same as Fig. 2, 3, but for $D=62$. Part (a,b) refers to $N_{ch} = 384$ ($\sigma = 0.03019$) and part (c,d) refers to $N_{ch} = 792$ ($\sigma = 0.06227$)



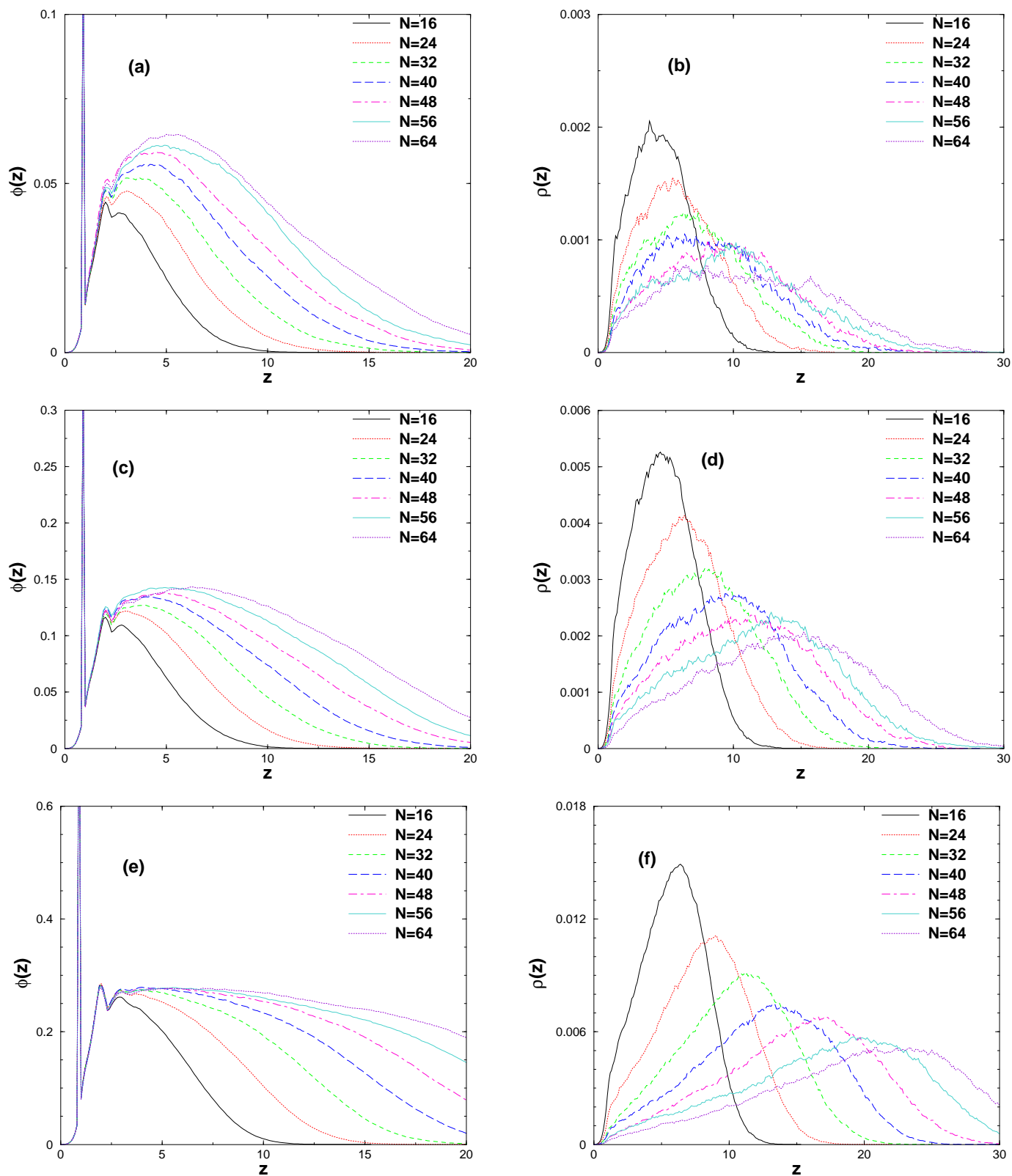
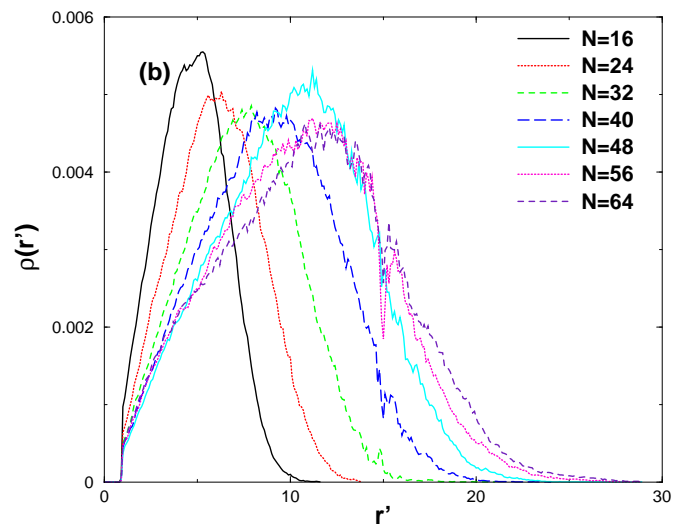
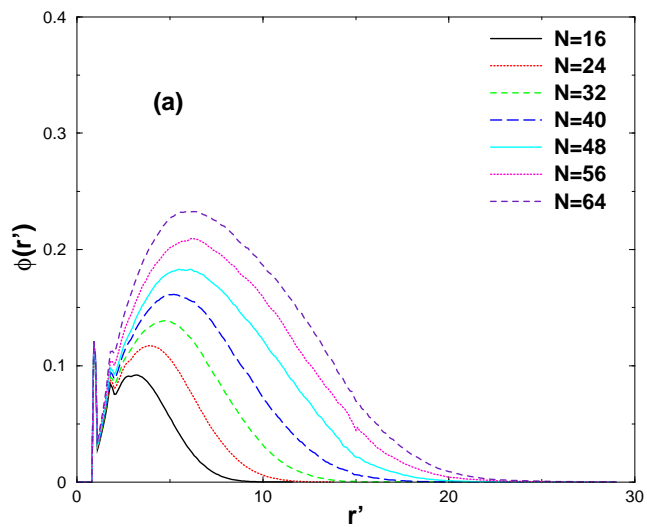


Figure 5: Same as Fig. 2 - 4, but for a flat substrate ($D = \infty$). Now the grafting wall is taken at the origin of the z -axis, which runs perpendicular to the grafting surface. Part (a,b) refers to the “mushroom” regime, ($N_{ch} = 36 \sigma = 0.01155$), while parts (c-f) refer to grafting densities comparable to Figs. 2 - 4, namely $N_{ch} = 100 \sigma = 0.03208$, part (c,d), and $N_{ch} = 289 \sigma = 0.10393$, part (e,f). parts a), c), e) show the monomer densities and parts b), d), f) the chain end distributions.

Figure 6: Distributions of all monomers of a chain, $\phi(r')$, part a, and of chain ends, $\rho(r')$, part b, plotted vs the distance r' from the grafting wall, for a cylindrical tube of diameter $D = 30$, grafting density $\sigma = 0.01$, and various chain lengths, as indicated in the figure.



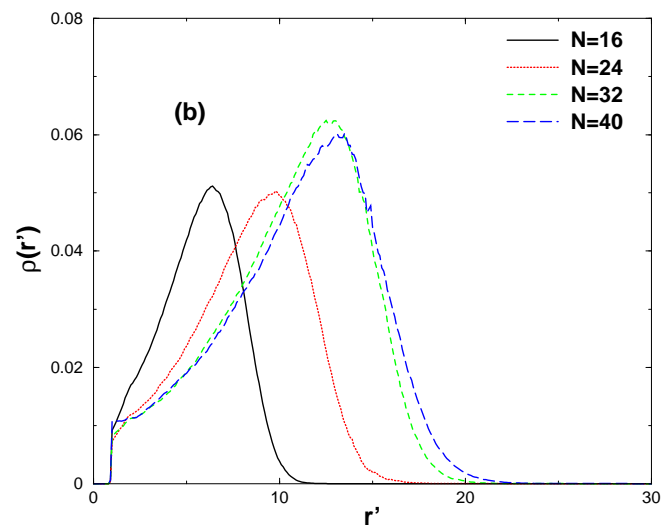
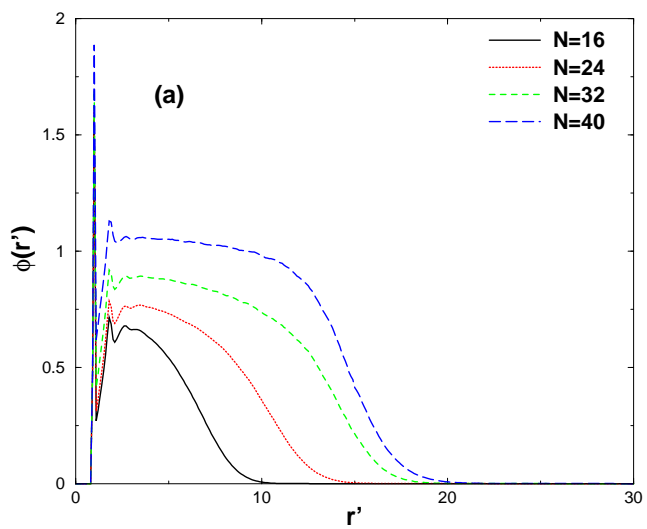
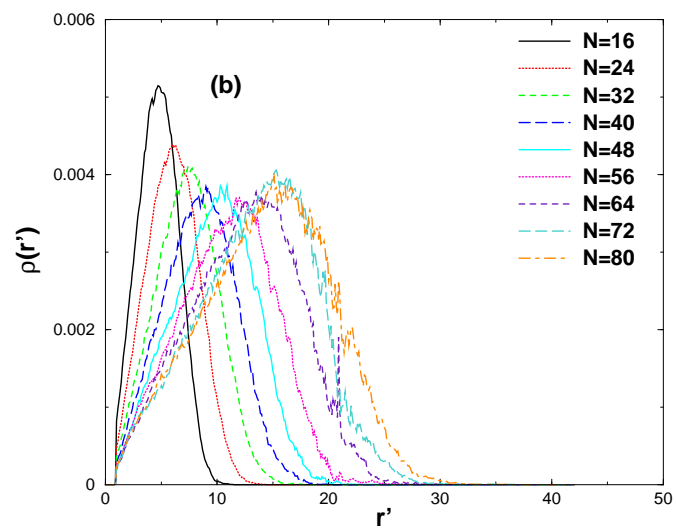
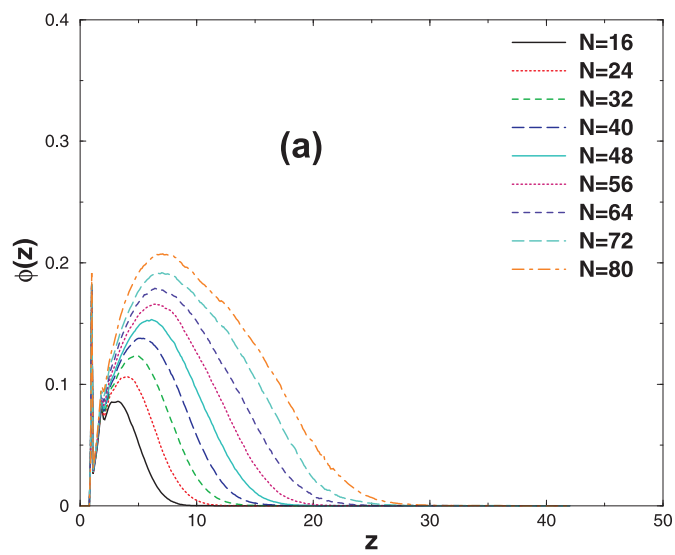


Figure 7: Same as Fig. 6, but for $\sigma = 0.09$.

Figure 8: Same as Fig. 6, but for $D = 42$.



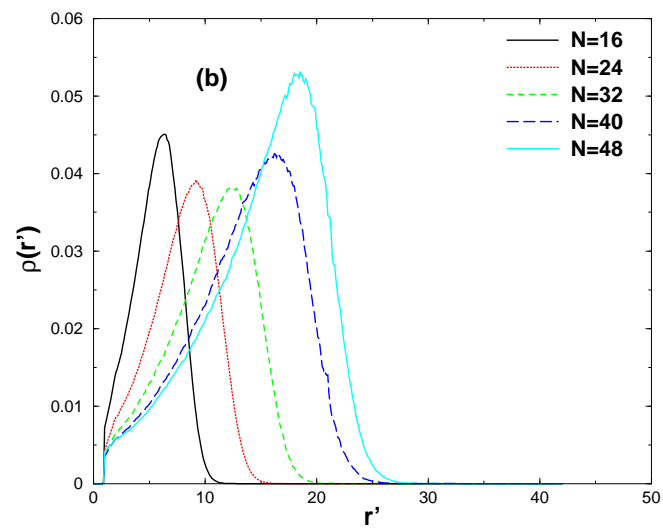
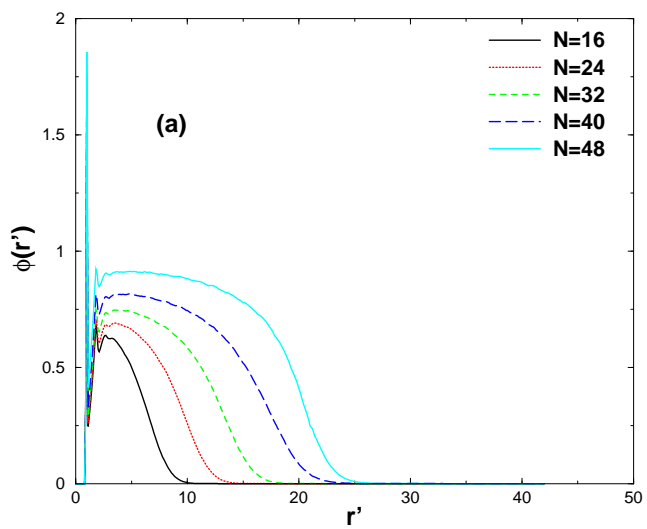


Figure 9: Same as Fig. 8, but for $\sigma = 0.09$.

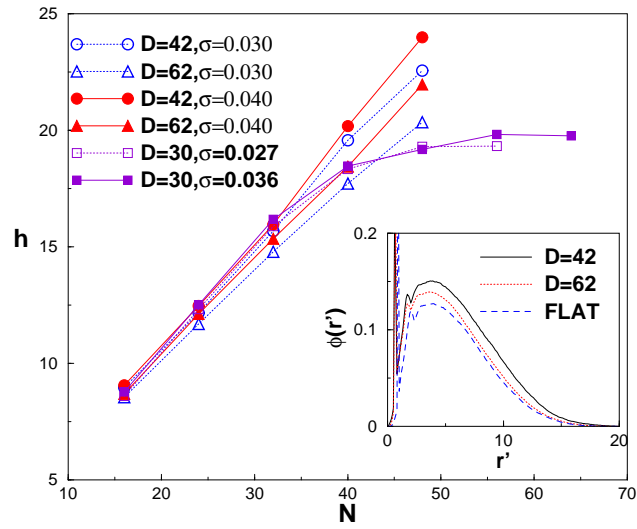
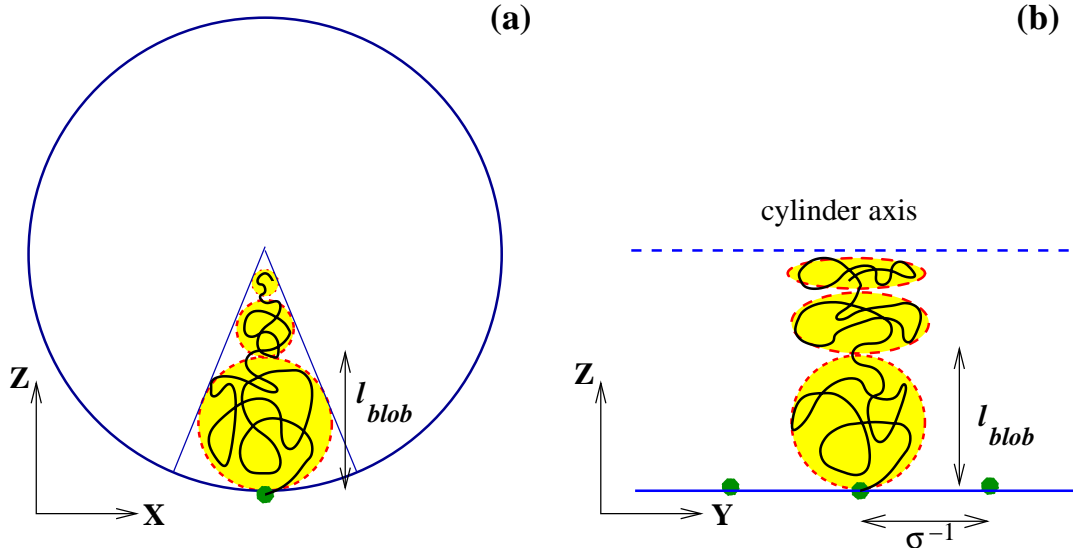


Figure 10: Brush height h plotted vs N for various diameters D and grafting densities σ , as indicated. Insert compares the density profiles $\phi(r')$ vs. r' for two choices of D at $\sigma = 0.03$ with the monomer density profile of a flat brush.

Figure 11: Schematic illustration of the generalization of the Alexander de Gennes blob picture for brushes to cylindrical geometry due to Sevick [22]. It is implied that each chain occupies in the zx -plane (cross-section of the cylinder) a conical sector (a), with the size l_{blob} of the outermost blob being delimited by the grafting density. In the zy -plane containing the cylinder axis, all blobs have a linear dimension l_{blob} along the y direction, but become progressively smaller in the z direction towards the cylinder axis (b). Note that our simulations rule out the validity of this simple picture, entropy favors that the chains share a much larger volume.



References

- [1] P. G. de Gennes, *J. Phys. (France)* **1976**, *37*, 1445.
- [2] P. G. de Gennes, *Macromolecules* **1980**, *13*, 1069.
- [3] S. Alexander, *J. Phys. (France)* **1977**, *38*, 983.
- [4] A. Halperin, M. Tirrell, and T. P. Lodge, *Adv. Polym. Sci.* **1991**, *100*, 31.
- [5] S. T. Milner, *Science* **1991**, *251*, 905.
- [6] R. C. Advincula, W. J. Brittain, K. C. Caster, and J. R uhe (eds.) “*Polymer Brushes*”, Wiley-VCH, Weinheim 2004.
- [7] A. N. Semenov, *Sov. Phys. JETP Lett.* **1985**, *61*, 733.
- [8] S. T. Milner, T. A. Witten, and M. E. Cates, *Europhys. Lett.* **1988**, *5*, 413.
- [9] S. T. Milner, T. A. Witten, and M. E. Cates, *Macromolecules* **1988**, *21*, 2610.
- [10] S. T. Milner and T. A. Witten, *J. Phys. (France)* **1988**, *49*, 1951.
- [11] T. Cosgrove, T. Heath, B. van Lent, F. Leermakers, and J. M. H. M. Scheutjens, *Macromolecules* **1988**, *20*, 1962.
- [12] A. M. Skvortsov, A. A. Gorbunov, V. A. Pavlushkov, E. B. Zhulina, O. V. Borisov, and V. A. Pryamitsin, *Polym. Sci. USSR Ser. A* **1988**, *20*, 1706.
- [13] E. B. Zhulina, V. A. Pryamitsin, and O. V. Borisov, *Polymer Sci. USSR Ser. A*, **1989**, *31*, 205.
- [14] S. T. Milner, Z. G. Wang, and T. A. Witten, *Macromolecules* **1989**, *22*, 489.
- [15] E. B. Zhulina, O. V. Borisov, and V. A. Pryamitsin, *J. Colloid Interface Sci.* **1990**, *137*, 495.
- [16] B. van Lent, R. Israels, J. M. H. H. Scheutjens, and G. J. Fleer, *J. Colloid Interface Sci.* **1990**, *137*, 380.
- [17] R. C. Ball, J. F. Marko, S. T. Milner, and T. A. Witten, *Macromolecules* **1991**, *24*, 693.
- [18] E. B. Zhulina, O. V. Borisov, V. A. Pryamitsin, and T. M. Birshtein, *Macromolecules* **1991**, *24*, 140.
- [19] C. M. Wijmans, J. M. H. M. Scheutjens, and E. B. Zhulina, *Macromolecules* **1992**, *25*, 2657.
- [20] C. M. Wijmans and E. B. Zhulina, *Macromolecules* **1993**, *26*, 7214.
- [21] N. Dan and M. Tirrell, *Macromolecules* **1993**, *26*, 637.
- [22] E. M. Sevick, *Macromolecules* **1996**, *29*, 6952.
- [23] C. Hiergeist and R. Lipowsky, *J. Phys. II (France)* **1996**, *6*, 1465.
- [24] E. N. Govorun and I. Erukhimovich, *Langmuir*, **1999**, *15*, 8392.
- [25] M. Manghi, M. Aubouy, C. Gay and C. Ligoure, *Eur. Phys. J. E.* **2001**, *5*, 519.

- [26] M. Murat and G. S. Grest, *Phys. Rev. Lett.* **1989**, *63*, 1074.
- [27] M. Murat and G. S. Grest, *Macromolecules* **1989**, *22*, 4054.
- [28] A. Chakrabarti and R. Toral, *Macromolecules* **1990**, *23*, 2016.
- [29] P.-Y. Lai and K. Binder, *J. Chem. Phys.* **1991**, *95*, 9288.
- [30] M. Murat and G. S. Grest, *Macromolecules* **1991**, *24*, 704.
- [31] G. S. Grest and M. Murat, *Macromolecules* **1993**, *26*, 3108.
- [32] J. Wittmer, A. Johner, J.-F. Joanny and K. Binder, *J. Chem. Phys.* **1994**, *101*, 4379.
- [33] K. Binder, P.-Y. Lai, and J. Wittmer, *Faraday Discuss.* **1994**, *98*, 97.
- [34] G. S. Grest and M. Murat, in: *Monte Carlo and Molecular Dynamics Simulations in Polymer Science*, edited by K. Binder, Oxford Univ. Press, New York **1995**, p. 476.; G. S. Grest, *Adv. Polym. Sci.* **1999**, *138*, 149.
- [35] K. Prochazka, *J. Phys. Chem.* **1995**, *99*, 14108.
- [36] I. Szleifer and M. Carignano, *Adv. Chem. Phys.* **1996**, *94*, 165; I. Szleifer and M. Carignano, *J. Chem. Phys.* **1995**, *102*, 8662.
- [37] P. Sotta, A. Lesne and J. M. Victor, *J. Chem. Phys.* **2000**, *112*, 1565.
- [38] T. Kreer, S. Metzger, M. Müller, K. Binder and J. Baschnagel, *J. Chem. Phys.* **2004**, *120*, 4012.
- [39] F. Tessier and G. W. Slater, *Macromolecules* **2005**, *38*, 6752; **2006**, *39*, 1250.
- [40] K. Binder, in: *Computational Modelling of Polymers*, edited by J. Bicerano, Marcel Dekker, New York, 1992, p. 221.
- [41] K. Binder, ed. “*Monte Carlo and Molecular Dynamics of Condensed Matter Systems*”, Societa Italiana di Fisica, Bologna 1996.
- [42] K. Binder and G. Ciccotti, eds. “*Monte Carlo and Molecular Dynamics of Condensed Matter Systems*”, Societa Italiana di Fisica, Bologna, 1996.
- [43] K. Binder and A. Milchev, *J. Computer-Aided Mater. Design* **2000**, *9*, 93.
- [44] M. Kotelyanskii and D. N. Theodorou, eds. “*Computer Simulation Methods for Polymers*”, Marcel Dekker, New York, 2004.
- [45] T. Kreer, M. H. Müser, K. Binder, and J. Klein, *Langmuir* **2001**, *17*, 7804.
- [46] P. J. Flory, “*Principles of Polymer Chemistry*”, Cornell University Press, Ithaca, N. Y., 1953.
- [47] M. Müller and L.-G. MacDowell, *Macromolecules* **2000**, *33*, 3902.
- [48] G. S. Grest and K. Kremer, *Phys. Rev. A* **1986**, *33*, 3628.
- [49] C. Bennemann, K. Binder, W. Paul, and B. Dünweg, *Phys. Rev. E* **1998**, *57*, 843.
- [50] I. Werning, M. Müller, and K. Binder, *Europhys. Lett.* **2005**, *71*, 639.

- [51] M. Meyyappan, ed. “*Carbon Nanotubes: Science and Applications*” CRC Press, Boca Raton, 2004
- [52] Z. N. Yu, H. Gao, W. Wu, H.X.Ge, and S. Y. Chou, *J. Vac. Sci. Technol. B* **2003**, *21*, 2874.
- [53] W. Reisner, K. J. Morton, R. Rühn, Y. M. Wang, Z. Yu, M. Rosen, J. C. Sturm, S. Y. Chou, E. Frey, and R. H. Austin, *Phys. Rev. Lett.* **2005**, *94*, 196101.
- [54] D. I. Dimitrov, A. Milchev, and K. Binder, *J.Chem.Phys.*(in press)